An Optoelectronic Oscillator for High Sensitivity Temperature Sensing

Yiping Wang, Jiejun Zhang, *Student Member, IEEE*, and Jianping Yao, *Fellow, IEEE*

***Abstract*— An optoelectronic oscillator (OEO) for high sensitivity temperature sensing is proposed and experimentally demonstrated. The oscillation frequency of the OEO is determined by a single passband microwave photonic filter (MPF) in the OEO loop, which is implemented using a broadband light source, a Mach–Zehnder interferometer (MZI), a dispersion compensating fiber, and a photodetector. One arm of the MZI is used as a sensing arm, which is exposed to temperature variations and the other arm is used as a reference arm. When the temperature is changed, the length difference between the two arms is changed, which leads to the change of the free spectral range of the MZI. Since the central frequency of the MPF is a function of the FSR, the oscillation frequency of the OEO is affected by the temperature variations. By measuring the frequency change, the temperature change to the sensing arm is estimated. The proposed approach is experimentally evaluated. High sensitivity temperature sensing with a sensitivity of 3.7 MHz/°C is experimentally demonstrated.**

***Index Terms*— Fiber optics sensor, Mach-Zehnder fiber interferometer, microwave photonics, optoelectronic oscillator.**

I. Introduction

In THE past few decades, numerous fiber-optic sensors have been proposed for measuring various physical and chemical parameters. The key advantages of fiber-optic sensors include immunity to electromagnetic interference, light weight, high sensitivity, and strong resistance to chemical erosion [1]. Among these measuring techniques, fiber-optic sensors based on a fiber-optic Mach–Zehnder interferometer (MZI) have attracted great attention because of the advantages of simple structure, easy fabrication, and low cost [2]. A fiber-optic MZI can be formed using two fiber couplers connected by two arms with unequal optical lengths. For sensing applications, one of the two arms is used as a sensing arm and the other is used as a reference arm. The sensing arm is exposed to external variations such as temperature while the reference arm is isolated from the external variations. The optical phase difference between the two arms of the MZI would change due to the length changes in the sensing arm resulted from the measurand changes. By analyzing the variations in the interference signal at the output of the MZI, the measurand could be determined.

However, a traditional MZI sensor using two fiber couplers usually has a low sensitivity since the interrogation is done in the optical domain using an optical spectrum analyzer (OSA). In addition, due to the poor resolution and low speed of an OSA, an MZI sensor based on an OSA also has a poor resolution and low speed. To increase the sensing performance, various new configurations and fabrication techniques have been exploited to construct a highly sensitive all-fiber MZI sensor. As far as a temperature sensor is concerned, these techniques include the use of a mismatched or misaligned core diameter MZI [3], a tapered fiber MZI [4], a microcavity-based MZI [5], a trench-structured MZI [6], and a fiber Bragg grating based MZI [7]. Many of these sensors, although having shown excellent performance, would be difficult to use in a practical system due to the complicated structure and high mechanical fragility. In addition, the interrogation of such an MZI sensor is still done in the optical domain using an OSA, which is again slow and has a poor resolution. Therefore, an MZI-based fiber-optic sensor with a high sensitivity, fast interrogation speed and good resolution is still an active research topic and has been heavily studied.

On the other hand, an optoelectronic oscillator (OEO) can be used in a fiber-optic sensor system to increase the sensitivity, interrogation speed and resolution [8], [9]. Various OEO-based fiber-optic sensors have been proposed, such as a refractive index sensor [10], a temperature sensor [11] and a transverse load sensor [12]. It is different from a fiber-optic sensor using an OSA to perform interrogation, an OEO-based sensor is interrogated by measuring the microwave frequency in the time domain, thus the speed is significantly increased. In addition, the frequency change can be precisely measured at an Hz resolution, which leads to an ultra-high sensitivity and resolution. The OEO-based sensors reported in [10] and [11] use the entire fiber loop as the sensing element, which may make point sensing impossible. In addition, the length of the fiber loop can be easily influenced by other environmental disturbances, deteriorating the sensing accuracy. In [12], the sensing element is a fiber Bragg grating (FBG). The size of an FBG is small and the sensing information will not be easily affected by the other environmental disturbances.

Manuscript received January 7, 2016; revised March 8, 2016; accepted April 12, 2016. Date of publication April 13, 2016; date of current version May 9, 2016. This work was supported by the Natural Sciences and Engineering Research Council of Canada. The work of Y. Wang was supported in part by the National Science Foundation of China under Grant 61307108.

Y. Wang is with the Microwave Photonics Research Laboratory, School of Electrical Engineering and Computer Science, University of Ottawa, Ottawa, ON K1N 6N5, Canada, and also with the School of Physics Science and Technology, Nanjing Normal University, Nanjing 210023, China.

J. Zhang is with the School of Electrical Engineering and Computer Science, University of Ottawa, Ottawa, ON K1N 6N5, Canada.

J. Yao is with the Microwave Photonics Research Laboratory, School of Electrical Engineering and Computer Science, University of Ottawa, Ottawa, ON K1N 6N5, Canada (e-mail: jpyao@eecs.uottawa.ca).

Color versions of one or more of the figures in this letter are available online at http://ieeexplore.ieee.org.

Digital Object Identifier 10.1109/LPT.2016.2553958

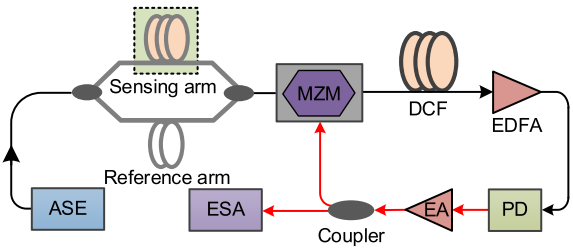

Fig. 1. Schematic of the proposed OEO based sensing system. ASE: amplified spontaneous emission. MZM: Mach–Zehnder modulator. DCF: dispersion compensating fiber. EDFA: erbium-doped fiber amplifier. PD: photodetector. EA: electrical amplifier. ESA: electrical spectrum analyzer.

However, since the oscillation frequency is directly related to the wavelength of the tunable laser source (TLS) used in the system, a small wavelength drift would lead to a large drift in the microwave frequency, which would cause a large error in the interrogation.

In this letter, we propose an MZI-based fiber-optic temperature sensor that is implemented using a fiber-optic MZI in conjunction with an OEO to increase the sensing sensitivity, interrogation speed and resolution. Since the OEO is implemented using a spectrum-sliced broadband light source, the dependence of the microwave frequency on the wavelength of the TLS is eliminated and the sensing accuracy is thus significantly increased. The fundamental concept of the proposed approach is to convert the free spectral range (FSR) change of the MZI to the frequency change of the microwave signal generated by the OEO. Since a small FSR change would lead to a large microwave frequency change, the performance in terms of the sensing sensitivity and resolution is significantly increased. In addition, the frequency can be measured in the time domain using a digital signal processing (DSP) module, the interrogation speed is also significantly increased. In the proposed system, the MZI is formed using two 1×2 fiber couplers with two arms with one being used as a sensing arm and the other as a reference arm. A broadband light wave from a broadband light source is sent to the MZI to tailor the spectrum of the broadband light wave to have a sinusoidal shape, which is then lunched to the OEO. It has been demonstrated that the frequency of the generated microwave signal at the output of the OEO is a function of the FSR of the MZI [13]. Therefore, by monitoring the microwave frequency change, the temperature change is measured. Thanks to the high speed and high resolution when measuring the microwave frequency using a DSP module, the proposed sensor would operate at an ultra-high speed and ultra-high interrogation resolution. The proposed approach is experimentally evaluated. A temperature sensor with a sensing sensitivity of 3.7 MHz/°C is experimentally demonstrated. In addition to the high speed, high resolution and high sensitivity, the proposed sensor is able to perform remote sensing since the MZI can be placed at a location that is far from the OEO loop, this is an added advantage to the proposed sensor.

II. Principle and Experimental Setup

Fig.1 illustrates the schematic of the proposed temperature sensing system. The light wave from a broadband amplified spontaneous emission (ASE) source is coupled into an MZI consisting of two 3-dB 1×2 couplers and two unequal-length arms. The two fiber arms of the MZI have a length difference of ΔL. The upper arm is used as a sensing arm and the lower arm as a reference arm. When the temperature applied to the sensing arm is changed, the length difference between the two arms is changed, which would lead to the change in the FSR of the MZI. Note that the spectra response of the MZI has a shape that is sinusoidal. The broadband light from the ASE source is sliced by the MZI, which lead to an amplitude tailored light wave with a sinusoidal envelope. The spectrum-sliced broadband light wave is then coupled into a Mach-Zehnder modulator (MZM), which is biased at the quadrature point. The modulated light wave is sent to a length of dispersive fiber, which is a dispersion compensating fiber (DCF) in our demonstration. After amplification by an erbium-doped fiber amplifier (EDFA), the light wave is sent to a photodetector (PD). The electrical signal at the output of the PD is amplified by an electrical amplifier (EA) and fed back to the MZM to form the OEO loop.

It is known that the joint operation of a sinusoidal-shaped broadband light wave, an MZM, a DCF and a PD corresponds to a single bandpass microwave photonic filter with its bandpass frequency determined by the FSR of the MZI, the dispersion of the DCF [13]. Mathematically, the center frequency of the passband of the MPF is given by [14],

$$f_0 = \frac{1}{D\Delta\lambda^0_{FSR}} = \frac{n_{eff}\Delta L_0}{D\lambda^2} \tag{1}$$

where D is the value of the group velocity dispersion (ps/nm) of the DCF, $\Delta\lambda^0_{FSR}$ is the original FSR of the MZI without the influence of a temperature change and can be expressed as $\Delta\lambda^0_{FSR} = \lambda^2/(n_{eff}\Delta L_0)$, where λ is the wavelength of the incident light wave, n_{eff} is the effective refractive index of the fiber core, and ΔL_0 is the original length difference between the two arms without experiencing a temperature change.

When the MPF is incorporated in the proposed OEO sensor system, a microwave signal with a frequency equal to the center frequency of the MPF will be generated. If the total dispersion of the fiber-optic link is fixed, the oscillating frequency of the microwave signal from the OEO can be uniquely determined by the FSR of the MZI, which is linearly proportional to the length difference between the two arms of the MZI. Therefore, when the temperature acted to the sensing arm is changed, the length difference between the two arms of the MZI is changed, and the FSR is also changed, which leads to the change in the microwave frequency.

Assuming that the length of the sensing arm that is subjected to a temperature perturbation is L_1, the final FSR of the MZI is given by

$$\begin{aligned}\Delta\lambda^1_{FSR} &= \frac{\lambda^2}{n\Delta L_0 + \Delta n L_1 + n\Delta L_1} \\ &= \frac{\lambda^2}{n\Delta L_0 + n\cdot\xi\cdot\Delta T\cdot L_1 + n\cdot\alpha\cdot\Delta T\cdot L_1} \\ &= \frac{\lambda^2}{n\Delta L_0 + (\xi+\alpha)\cdot\Delta T\cdot n\cdot L_1}\end{aligned} \tag{2}$$

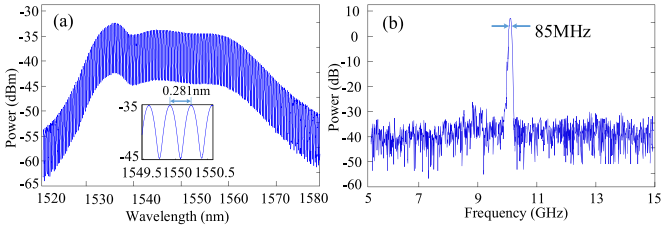

Fig. 2. (a) Optical spectrum measured at the output of the MZI. Inset: zoom-in view of the sliced spectrum. (b) Measured frequency response of the single passband MPF.

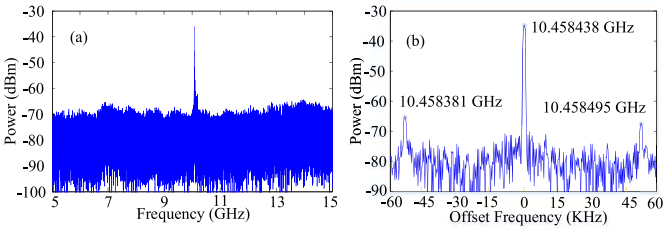

Fig. 3. (a) Electrical spectrum of the generated 10.458 GHz microwave signal at room temperature, here the resolution bandwidth (RBW) is 1.5MHz. (b) Zoom-in view of the signal (the RBW is 1 KHz).

where α ($\sim 0.55\times10^{-6}$/°C) is the thermal expansion coefficient of silica and ξ ($\sim 6.45\times10^{-6}$/°C) is the thermo-optic coefficient representing the temperature dependence of the refractive index. By using (1) and (2), the relationship between the induced central frequency shift of the OEO and the applied temperature can be expressed as

$$\Delta f = \frac{1}{D\Delta\lambda^{1}_{FSR}} - \frac{1}{D\Delta\lambda^{0}_{FSR}} = \frac{1}{D\lambda^{2}}(\eta+\alpha)\cdot\Delta T\cdot n\cdot L_1 \quad (3)$$

From (3), we can see the microwave frequency shift is linearly proportional to the temperature change, thus by measuring the frequency change the temperature change can be estimated.

III. Experimental Results

An experiment is carried out based on the setup shown in Fig. 1. An ASE source with a spectral width of 30 nm is used as the broadband optical source. The MZI is fabricated by fusion-splicing two 3-dB 1×2 couplers with two arms. The original length difference between the two arms is controlled to be 4 mm, which is done by using an optical vector analyzer (OVA, Luna OVA 4000) to monitoring the FSR.

We first measure the spectrum of the sliced light wave. A broadband light wave is generated by an ASE source which is an EDFA with no input optical signal. The sliced spectrum measured at the output of the MZI is shown in Fig. 2(a). The inset gives a zoom-in view of the sliced spectrum. As shown in Fig. 2(a), the ASE light source is sliced into more than 100 channels and the channel spacing or the FSR is 0.281nm. The sliced light wave is then sent to the MZM, where it is modulated by a microwave signal applied to the MZM via the RF port. The modulated light wave is sent to the DCF. The DCF we used is a packaged DCF module with environmental isolation (Lucent DK 340), the use of which could minimize the effects of temperature, strain, and vibrations from the environment. The DCF has a value of dispersion of 339 ps/nm. After passing through the DCF and amplified by the EDFA, the optical signal is converted to a microwave signal and amplified by the EA. We then measure the frequency response of the MPF without closing the OEO loop, which is done by using a vector network analyzer (VNA, Agilent E8364A) with the RF port of the MZM as the input port of the MPF and the output port of the EA as the output port of the MPF. Fig. 2(b) shows the measured frequency response of the MPF. As can be seen the passband frequency is located around 10.46 GHz, which agrees well with the theoretical value of 10.50 GHz calculated based on (1). The 3-dB bandwidth of the frequency resonance is 85 MHz. The extinction ratio of the MPF is more than 30 dB, which is large enough to suppress the undesirable side modes in the OEO.

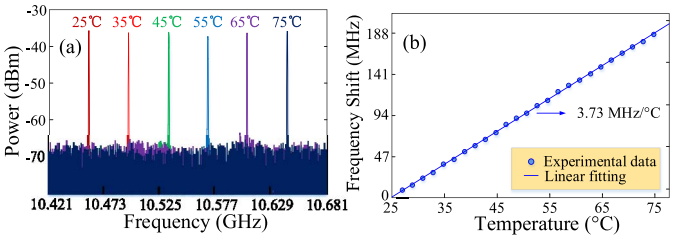

Fig. 4. (a) Superimposed electrical spectra of the generated microwave signal at different temperatures. (b) Measured oscillation frequency shift as a function of the applied temperature to the sensing arm from 25°C to 75°C with a step of 2°C.

Then, we then close the OEO loop. By controlling the gains of the EDFA and EA to make the OEO net loop gain higher than 0 dB, the OEO will start to oscillate. Fig. 3(a) shows the spectrum of the generated 10.458 GHz microwave signal at a room temperature measured by an electrical spectrum analyzer (ESA, Agilent E4448A). Fig. 3(b) provides a zoom-in view of the spectrum of the generated microwave signal. Several peaks are observed in Fig. 3(b), which are resulted from the side modes of the OEO. The first side mode peak is located at an offset frequency of 57 kHz, which indicates the FSR of the OEO loop is 57 kHz corresponding to a length of 3.6 km for the global OEO loop. It should be noted that although the different modes are not completely filtered out by the MPF, the main oscillation mode is predominant to meet the requirement for accurate sensing. In addition, by properly decreasing the OEO net loop gain, we could further suppress the side modes.

Finally, temperature sensing is evaluated. To do so, we use a 30-cm fiber in the sensing arm which is placed in a temperature controlled water tank. When the temperature of the water is increased from 25°C to 70°C, the microwave frequency at different temperature points is recorded. Fig. 4(a) shows the superimposed spectra of the generated microwave signal at different temperatures. As can be seen in Fig. 4(a), the microwave frequency is shifted to a higher frequency from 10.458 GHz to 10.643 GHz as the temperature is increased from 25°C to 75°C. This phenomenon indicates that the optical

length in the sensing arm is increased as the temperature is increased, which leads to the change in the length difference of the two arms and the FSR, which leads to the change in the microwave frequency.

Fig. 4(b) shows the measured oscillation frequency shift as a function of the applied temperature on the sensing arm from 25°C to 75°C with a step of 2°C. The sensitivity by linearly fitting the measured data in Fig. 4(b) is 3.73 MHz/°C, which is much higher than that using a similar temperature sensor based on an OEO [11]. This is because in our proposed sensing system the sensing element is a section of optical fiber in the MZI, while in [12] the sensing element is an optical fiber which constitutes the entire loop of the OEO. Since the MZI structure is more sensitive to a temperature change, a higher sensitivity is ensured. Note that the environmental temperature change and environmental vibrations may affect the unpackaged part of the OEO, which may change the length of the entire OEO loop, and accordingly, the FSR of the OEO loop and the oscillation frequency. Therefore, the stability of the OEO will decrease and mode hopping may occur. However, according to the oscillation theory of an OEO, the uncertainty of the oscillation frequency is less than the FSR of the OEO. Since the FSR of the OEO in our experiment is 57 KHz and the temperature sensitivity is 3.7 MHz/°C, the uncertainty of the oscillation frequency can hardly affect the temperature measurement. Therefore, we can conclude that the proposed temperature sensor is independent of any other environmental changes, including a temperature change induced to the 3.6 km OEO loop.

The stability, accuracy and repeatability of the proposed temperature sensor are also evaluated. Theoretically, the resolution of the proposed temperature sensor is limited by the FSR of the OEO loop. For the demonstrated OEO sensor, the FSR is measured to be about 57 KHz, which corresponds to a resolution of 0.015°C. But in practice, it is difficult to achieve such a high resolution because of the instability of the OEO. To evaluate the stability, the system was allowed to operate in a room environment for a period of 30 minutes. It is demonstrated that the maximum frequency offsets in the oscillation frequency is within 300 KHz, which corresponds to a temperature measurement accuracy of 0.08°C. Note that the accuracy of the digital thermometer used in our experiment is only 0.1°C, which limits the measurement accuracy in our experiment to be 0.1°C. In order to demonstrate the repeatability of the proposed sensor, we perform the temperature test at 30°C and 40°C alternately for ten times and record the data. The results indicate that the repeatability error is less than 0.02%.

IV. Discussion and Conclusion

It should be noted that if the sensor is interrogated through directly monitoring the FSR change by use an OSA, the sensitively will be extremely low. Based on (2), a change in temperature of 1°C will lead to a change in FSR of less than 1 pm, which is too low to be accurately measured by an OSA. On the other hand, a change in FSR of 1 pm can lead to a change in the microwave frequency by 37.38 MHz, which is very large and can be easily and accurately measured.

It is worth noting that the proposed sensing system could also be used to measure other parameters such as a strain. If the sensing element is replaced by a Fabry–Pérot (F-P) interferometric cavity [15], [16], the proposed sensor can also be used as a pressure and refractive index sensor.

In conclusion, we have proposed and experimentally demonstrated a temperature sensor with ultra-high resolution and sensitivity based on an OEO. The fundamental principle of the work was to translate the FSR change of the MZI to the frequency shift of the generated microwave signal by the OEO. The experiment results showed that a high sensitivity of 3.73 MHz/°C was achieved for a sensing fiber with a length of 30 cm. The proposed sensor system exhibits several important features, including simple structure, low cost, and high temperature sensitivity. It can also be used for remote sensing.

References

[1] T. G. Giallorenzi *et al.*, "Optical fiber sensor technology," *IEEE Trans. Microw. Theory Techn.*, vol. 30, no. 4, pp. 472–511, Apr. 1982.

[2] E. Udd, "Fiber optic smart structures," in *Fiber Optic Sensors: An Introduction for Engineers and Scientists*. Hoboken, NJ, USA: Wiley, 1991.

[3] L. V. Nguyen, D. Hwang, S. Moon, D. S. Moon, and Y. Chung, "High temperature fiber sensor with high sensitivity based on core diameter mismatch," *Opt. Exp.*, vol. 19, no. 15, pp. 11369–11375, Jul. 2008.

[4] P. Lu, L. Men, K. Sooley, and Q. Chen, "Tapered fiber Mach–Zehnder interferometer for simultaneous measurement of refractive index and temperature," *Appl. Phys. Lett.*, vol. 94, no. 13, pp. 131110–131113, Apr. 2009.

[5] L. Jiang, J. Yang, S. Wang, B. Li, and M. Wang, "Fiber Mach–Zehnder interferometer based on microcavities for high-temperature sensing with high sensitivity," *Opt. Lett.*, vol. 36, no. 19, pp. 3753–3755, Sep. 2011.

[6] Y. Wang, Y. Li, C. Liao, D. N. Wang, M. Yang, and P. Lu, "High-temperature sensing using miniaturized fiber in-line Mach–Zehnder interferometer," *IEEE Photon. Technol. Lett.*, vol. 22, no. 1, pp. 39–41, Jan. 1, 2010.

[7] C. R. Liao, Y. Wang, D. N. Wang, and M. W. Yang, "Fiber in-line Mach–Zehnder interferometer embedded in FBG for simultaneous refractive index and temperature measurement," *IEEE Photon. Technol. Lett.*, vol. 22, no. 22, pp. 1686–1688, Nov. 15, 2010.

[8] X. S. Yao and L. Maleki, "Optoelectronic microwave oscillator," *J. Opt. Soc. Amer. B*, vol. 13, no. 8, pp. 1725–1735, 1996.

[9] X. S. Yao and L. Maleki, "Optoelectronic oscillator for photonic systems," *IEEE J. Quantum Electron.*, vol. 32, no. 7, pp. 1141–1149, Jul. 1996.

[10] L. D. Nguyen, K. Nakatani, and B. Journet, "Refractive index measurement by using an optoelectronic oscillator," *IEEE Photon. Technol. Lett.*, vol. 22, no. 12, pp. 857–859, Jun. 15, 2010.

[11] Y. Zhu, X. Jin, H. Chi, S. Zheng, and X. Zhang, "High-sensitivity temperature sensor based on an optoelectronic oscillator," *Appl. Opt.*, vol. 53, no. 22, pp. 5084–5087, Aug. 2014.

[12] F. Kong, W. Li, and J. Yao, "Transverse load sensing based on a dual-frequency optoelectronic oscillator," *Opt. Lett.*, vol. 38, no. 14, pp. 2611–2613, Jul. 2013.

[13] J. Mora *et al.*, "Photonic microwave tunable single-bandpass filter based on a Mach–Zehnder interferometer," *J. Lightw. Technol.*, vol. 24, no. 7, pp. 2500–2509, Jul. 2006.

[14] J. H. Lee and Y.-M. Chang, "Detailed theoretical and experimental study on single passband, photonic microwave FIR filter using digital micromirror device and continuous-wave supercontinuum," *J. Lightw. Technol.*, vol. 26, no. 15, pp. 2619–2628, Aug. 1, 2008.

[15] A. Wang, H. Xiao, J. Wang, Z. Wang, W. Zhao, and R. G. May, "Self-calibrated interferometric-intensity-based optical fiber sensors," *J. Lightw. Technol.*, vol. 19, no. 10, pp. 1495–1501, Oct. 2001.

[16] T. Wei, Y. Han, Y. Li, H.-L. Tsai, and H. Xiao, "Temperature-insensitive miniaturized fiber inline Fabry–Perot interferometer for highly sensitive refractive index measurement," *Opt. Exp.*, vol. 16, no. 8, pp. 5764–5769, Apr. 2008.